Urbanization and Climate Change: An Examination of Nonstationarities in Urban Flooding

LONG YANG

Department of Hydraulic Engineering, Tsinghua University, Beijing, China, and Department of Civil and Environmental Engineering, Princeton University, Princeton, New Jersey

JAMES A. SMITH, DANIEL B. WRIGHT, AND MARY LYNN BAECK

Department of Civil and Environmental Engineering, Princeton University, Princeton, New Jersey

GABRIELE VILLARINI

IIHR—Hydroscience and Engineering, The University of Iowa, Iowa City, Iowa

FUQIANG TIAN AND HEPING HU

Department of Hydraulic Engineering, Tsinghua University, Beijing, China

(Manuscript received 29 June 2012, in final form 25 May 2013)

ABSTRACT

The authors examine the hydroclimatology, hydrometeorology, and hydrology of flooding in the Milwaukee metropolitan region of the upper midwestern United States. The objectives of this study are 1) to assess nonstationarities in flood frequency associated with urban transformation of land surface properties and climate change and 2) to examine how spatial heterogeneity in land surface properties and heavy rainfall climatology interact to determine floods in urbanizing areas. The authors focus on the Menomonee River basin, which drains much of the urban core of Milwaukee, and the adjacent Cedar Creek basin, where agricultural land use dominates. Results are based on analyses of bias-corrected, high-resolution (1-km^2 spatial resolution and 15-min time resolution) radar rainfall fields that are developed using the Hydro-NEXRAD system, rainfall observations from a network of 21 rain gauges in the Milwaukee metropolitan region, and discharge observations from 11 U.S. Geological Survey stream gauging stations. Both annual flood peak magnitudes and annual peaks over threshold flood counts have increased for the Menomonee River basin during the past five decades, and these trends are accompanied by a transition of flood events dominated by snowmelt (March–April floods) to a regime in which warm season thunderstorms are the dominant flood-producing agents. The frequency of heavy rainfall events has increased significantly. The spatial distribution of rainfall for flood-producing storms in the Milwaukee study region exhibits striking spatial heterogeneity, with a maximum in the central portion of the Menomonee River basin. Storm event hydrologic response is determined by the interactions of spatial patterns of urbanization and rainfall distribution in the Menomonee River basin.

1. Introduction

In this paper, we examine the hydroclimatology, hydrometeorology, and hydrology of floods through analyses centered on the Menomonee River basin in the Milwaukee, Wisconsin, metropolitan region (Fig. 1). The Menomonee River basin, which has a drainage area of 319 km^2, exhibits heterogeneous land use and land cover, including some of the most heavily urbanized portions of Milwaukee (Zhang and Smith 2003). Adjacent to the northern boundary of the Menomonee River basin is the Cedar Creek basin (Fig. 1), which has nearly the same basin area (311 km^2) but is predominantly agricultural. Cedar Creek will serve as a ''reference'' watershed for hydroclimatological analyses of flooding in the Menomonee River, providing a representation of the regional

Corresponding author address: Long Yang, New Hydraulic Building, Tsinghua University, Beijing 100084, China.
E-mail: yanglong86123@hotmail.com

DOI: 10.1175/JHM-D-12-095.1

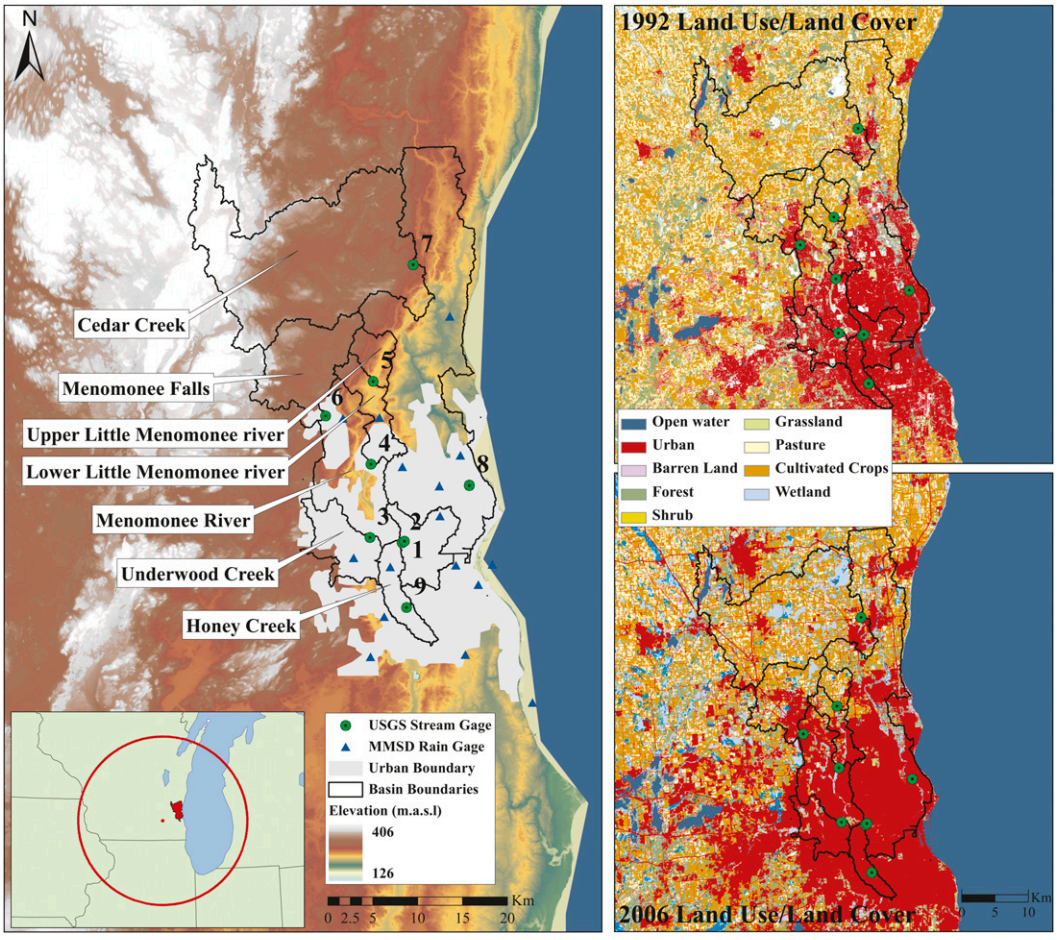

FIG. 1. (left) Location of the study area in the upper Midwest, USGS streamflow gauges, and MMSD rain gauges. Milwaukee metropolitan region is shaded in gray. Basin boundaries for the Menomonee River basin, Cedar Creek basin, and their subbasins are shown in black lines. Red circle indicates the 200-km radius from the KMKX WSR-88D radar. (top right) NLCD1992 land use map. (bottom right) NLCD2006 land use map. USGS stream gauge IDs: 1) 04087120, 2) 04087119, 3) 04087088, 4) 04087070, 5) 04087050, 6) 04087030, 7) 04086500, 8) 04087000, and 9) 04087100.

flood response of southern Wisconsin, in which agricultural land use dominates.

Previous studies have examined changes in hydrological response of watersheds due to land use change and climate change. Paired watershed studies, which can yield direct evidence of impacts (e.g., Changnon and Demissie 1996; Hewlett and Helvey 1970), provide a useful approach to assessing changing responses. The combined analyses of hydrologic response for the Menomonee River and Cedar Creek basins in this study draw on approaches developed in paired watershed studies. Statistical and hydrologic modeling advances have also played an important role in assessing changing flood response of watersheds (e.g., Hejazi and Markus 2009; Villarini et al. 2009b, 2011a, 2013a; Smith et al. 2010; Chung et al. 2011; Cuo et al. 2009; Franczyk and Chang 2009; Claessens et al. 2006; Semadeni-Davies et al. 2008a,b; Praskievicz and Chang 2009). In this study, we draw on statistical approaches for assessing nonstationarities in flood records and rainfall records, motivated in part by the observation of Milly et al. (2008), that ''stationarity is dead'' (for cautionary discussion of the demise of stationarity, see, e.g., Villarini et al. 2009a).

A central theme of this study is that spatial heterogeneities in land surface processes associated with runoff production and the climatology of heavy rainfall interact to determine the spatial and temporal properties of floods. Changes in the regional climatology of heavy rainfall are potentially linked to large-scale warming (e.g., Solomon et al. 2007; Easterling et al. 2000; Voss et al. 2002), especially as it affects water vapor in the atmosphere (e.g., Held and Soden 2006). Changes in the heavy

rainfall climatology for the Milwaukee region, and other urban areas around the world, are also potentially linked to urban modification of regional climate through urban heat island (UHI), urban canopy, and urban aerosol effects (as reviewed by Shepherd 2005; Collier 2005; Lowry 1998). Urban modification of the regional precipitation climatology is an important issue examined in this study.

Previous studies have pointed to increasing trends in rainfall over the midwestern United States (Karl and Knight 1998; Angel and Huff 1997; Lettenmaier et al. 1994; Kunkel et al. 1999). Villarini et al. (2011b) analyzed annual maximum daily rainfall accumulation for 221 rain gauges in the Midwest and found a slight tendency toward increasing trends. More recently, Villarini et al. (2013b) found increasing trends in the number of days with rainfall accumulation exceeding the 95th percentile over large areas of the upper Midwest, including Wisconsin.

It is well established, both theoretically and from observations, that urbanization can modify regional climate, including precipitation. Urban modification of the regional precipitation climatology has been reported in numerous empirical studies around the world (e.g., Changnon et al. 1971; Changnon 1980; Shepherd et al. 2002; Mote et al. 2007; Dixon and Mote 2003) and numerical modeling studies have provided insights to physical mechanisms at play (e.g., Yang et al. 2010; Zhang et al. 2009; Bornstein and Lin 2000; Lei et al. 2008; Miao et al. 2011). Smith et al. (2012) and Wright et al. (2012) have examined the fingerprints of urbanization on regional rainfall climatology based on long-term, high-resolution radar rainfall datasets over the Baltimore and Atlanta metropolitan regions, respectively, and presented analyses suggesting changes to the ''extremes'' of the regional rainfall climatology. In these settings, the impact of urbanization on heavy rainfall climatology is also linked to natural heterogeneities of terrain features (e.g., Ntelekos et al. 2008; Wright et al. 2012). The Milwaukee metropolitan region is located on the western boundary of Lake Michigan, which plays a key role in the local rainfall climatology. Urban modification of heavy rainfall for this region, as for many urban regions around the world (Changnon 1980; Lo et al. 2007; Shepherd et al. 2010; Lin et al. 2011; Cheng and Chan 2012), must be examined in the broader context of land–water–atmosphere interactions. This study will provide evidence for urban impacts on rainfall and lay a foundation for future numerical modeling studies.

Merz (2003) found that flood frequency distributions in Austria can be represented as ''mixtures'' of different flood-producing agents and that these mixtures are strongly linked to seasonally varying floods (see also Smith et al. 2011). Their results highlight the utility of examining the seasonality of floods, which can reflect the dominant flood-producing mechanisms and provide avenues for investigating the impacts of changes in climate and land use on flood frequency (Sivapalan 2005). Previous studies have shown that warm season thunderstorm systems become the dominant flood agents in some environments because of the changes in land surface properties associated with urbanization (e.g., Ntelekos et al. 2007; Doswell et al. 1996; Baeck and Smith 1998; Smith et al. 2005). In this study, we will further examine the role of warm season thunderstorm systems as urban flood agents.

Analyses of flooding and heavy rainfall presented in section 3 are motivated by the following hypotheses.

1) Changes in land surface processes associated with urbanization transform the dominant flood-producing agents from winter/spring snowmelt to warm season [June–August (JJA)] thunderstorm systems. These warm season thunderstorm systems are increasing in frequency and intensity, implying a component of nonstationarity in floods associated with climate change.
2) Flood peaks in nonurban areas are linked to snowmelt; in these basins, there is not a significant long-term trend in flood magnitudes, but temperature increases may lead to earlier occurrences of flood peaks during the year.
3) Nonstationarities in urban flood frequency reflect the complex interplay of changing hydrologic responses and regional heavy rainfall climatology.
4) Urbanization influences the regional rainfall climatology by altering the spatial distribution of heavy rainfall.

In this paper, we examine the evidence for each of these hypotheses and synthesize the changing flood response in a heterogeneous region that has experienced significant urbanization over the past five decades. We do not provide complete answers to these hypotheses, but attempt to provide directions that will help in developing methods that are necessary to obtain more definitive answers.

The methodology used to examine these hypotheses is based on analyses of streamflow and rainfall observations, for which there are exceptional resources in the Milwaukee area. We utilize long-term daily discharge observations from U. S. Geological Survey (USGS) stream gauging stations, as well as high temporal resolution (5–15 min) discharge observations for storm event analyses. We use composite rainfall fields for the Wisconsin region that we developed using the Hydro-NEXRAD system (e.g., Seo et al. 2010; Krajewski et al. 2010; Wright et al. 2012; Smith et al. 2012) at 15-min temporal resolution and 1-km horizontal scale for hydrometeorological and hydrologic analyses. The high-resolution radar

TABLE 1. Details of land use types in 1992 and 2006 for Menomonee River and Cedar Creek Basins. Land use data are obtained from NLCD.

	Cedar Creek basin			Menomonee River basin		
Types	1992 (%)	2006 (%)	Change	1992 (%)	2006 (%)	Change
Urban land	4	14	10	45	65	20
Forest	16	12	−4	13	7	−6
Cultivated crops	70	55	−15	37	20	−17
Other	10	19	9	5	8	3

rainfall fields provide a detailed representation of spatial and temporal variability of rainfall over urban areas (e.g., Baeck and Smith 1998; Smith et al. 1996a; Ciach and Krajewski 1999; Borga et al. 2002).

The paper is organized as follows. In section 2, we introduce the study region and the data utilized in this study, including stream gauging observations, rain gauge records, and radar rainfall data, as well as the algorithms used to develop bias-corrected radar rainfall fields. In section 3 we present analyses of nonstationarity of floods from three perspectives: hydroclimatology (section 3a), hydrometeorology (section 3b), and hydrology (section 3c). A discussion is presented in section 4, followed by a summary and conclusions in section 5.

2. Data and study region

The Menomonee River basin (Fig. 1), which drains a large portion of the Milwaukee metropolitan region, exhibits large contrasts in land use/land cover and topography. Elevation ranges from about 100 to more than 400 m MSL. A significant topographic transition zone can be seen in the Menomonee River valley, with higher elevations to the west and lakeside plains to the east. Much of the metropolitan region is located along this transition zone. On the eastern boundary of the basin is Lake Michigan, which is also included in our study domain.

The two land use datasets used in this study were obtained from the National Land Cover Dataset (NLCD) (Fig. 1, right; see http://www.mrlc.gov/ for more information) and reflect conditions for 1992 and 2006. Table 1 presents the main land use types and the percentage changes from 1992 to 2006. The Menomonee River basin has experienced major urban transformations during the past two decades, with the total urban fraction increasing from 45%–65%. The Cedar Creek basin remains largely agricultural, but has a small fraction of urbanized land (see discussion in section 3 on urbanization impacts on annual flood counts).

Although the Menomonee River basin is heavily urbanized, its subbasins exhibit large variability in land use (Table 2). Honey Creek and Underwood Creek are the most densely urbanized with 100% and 92% urban ratios, respectively. The Little Menomonee River and Menomonee Falls subbasins exhibit dense urbanization near their outlets. Less than 20% of the upper Little Menomonee River basin is urban; the remainder is forest and other nonurban land use types.

Discharge data from USGS stream gauging stations play a central role in this study. Analyses utilize instantaneous discharge data at 5–15-min resolution (linearly interpolated to uniform 1-min time interval for all stations), annual peak data, and mean daily discharge data from nine stations over the Menomonee River and Cedar Creek basins [station identifiers (IDs) are shown in the caption of Fig. 1]. The instantaneous discharge data are available for several stations from 1986 to 2010, while the others have data only after 2000. Most of the stations have daily discharge observations covering the period from 1962 to 2010. Cedar Creek at Cedarburg (USGS ID 04086500) has longer records, beginning in

TABLE 2. Summary of land use types for the subbasins of Menomonee River basin in 2006. Land use data are obtained from the NLCD.

	Land use ratios over five subbasins (%)				
Land use types	Honey Creek	Underwood Creek	Lower Little Menomonee River	Menomonee Falls	Upper Little Menomonee River
Developed, open space	10	32	8	8	6
Developed, low intensity	48	40	25	19	10
Developed, medium intensity	33	13	15	6	0
Developed, high intensity	9	7	7	3	0
Urban total	100	92	55	36	16
Forests	0	3	11	10	9
Cultivated Crops	0	2	22	43	65
Other	0	3	12	11	10
Total Area (km^2)	30.2	58.8	72.5	92.6	26.6

TABLE 3. Summary of the 18 largest floods over Menomonee River basin. NA denotes missing data.

Date	Peak Discharge ($m^3 s^{-1} km^{-2}$)	Total runoff (mm)	Total rainfall (mm)	Runoff ratio (-)
21 Jun 1997	1.21	84	85	0.99
6 Aug 1998	1.15	48	116	0.41
7 Jun 2008	1.12	98	165	0.59
19 Jun 2009	1.06	33	55	0.59
22 Jul 2010	0.96	76	141	0.54
15 Jul 2010	0.87	35	103	0.34
8 Jun 2008	0.67	32	32	1.00
21 Jul 1999	0.56	23	35	0.66
2 Jul 1997	0.48	14	18	0.82
9 Jul 2006	0.48	6.1	22	0.27
16 Jun 1996	0.47	43	74	0.58
4 Jul 2004	0.46	11	48	0.22
20 Jun 2009	0.44	1.5	NA	NA
15 Jun 2010	0.44	8.2	13	0.64
17 Jun 1996	0.43	4.5	8.9	0.51
13 Jun 1999	0.43	23	24	0.96
12 Sep 2006	0.41	7.9	16	0.48
9 Jul 1999	0.39	3.9	13	0.31

1932. Mean daily discharge observations are converted to peaks-over-threshold (POT) flood data for further analysis (see section 3a for additional details).

The Milwaukee Metropolitan Sewerage District (MMSD) maintains a network of 21 rain gauges with hourly rainfall observations starting in 1993. We use rain gauge observations to directly examine the rainfall climatology over the study region and to carry out bias correction for radar rainfall fields. In addition, cloud-to-ground (CG) lightning data from the National Lightning Detection Network (NLDN) are also used in this study to examine the spatial patterns of warm season thunderstorms over the study area. CG lightning data have been used in previous studies for climatological analyses of lightning and thunderstorms over the United States (e.g., Tapia et al. 1998; Carey and Rutledge 2003; Carey et al. 2003; Bentley and Stallins 2005; Ntelekos et al. 2007), and in particular, for examining urban modification of thunderstorms (see Shepherd 2005 for a review).

Radar rainfall fields are derived from volume scan reflectivity observations from the KMKX Weather Surveillance Radar-1988 Doppler (WSR-88D) radar located in Milwaukee, Wisconsin (see Fig. 1, left, for location). We use the Hydro-NEXRAD processing system to convert three-dimensional volume scan reflectivity fields in a polar coordinate system to two-dimensional surface rainfall fields in a Cartesian coordinate system. Quality control algorithms used for the rainfall fields include detection and removal of anomalous propagation (AP) returns (Steiner and Smith 2002) and hail detection and mitigation (Fulton et al. 1998; Baeck and Smith 1998). Conversion of reflectivity to rainfall rate is based on the default National Weather Service (NWS) Z–R relationship: $R = aZ^b$, where R is rain rate ($mm\,h^{-1}$), Z is radar reflectivity factor ($mm^6\,m^{-3}$), and the Z–R parameters take the values $a = 0.017$ and $b = 0.714$ (Fulton et al. 1998). The rainfall accumulation algorithm converts rainfall rate fields on irregular volume scan times (5–6-min time interval) to a regular 15-min time interval. The rainfall mapping algorithm converts rainfall fields from a 2D polar coordinate system to the Super–Hydrologic Rainfall Analysis Project (HRAP) coordinate system, a Cartesian coordinate system with horizontal resolution of approximately 1 km (Reed and Maidment 1999; Seo et al. 2010).

The radar rainfall fields analyzed in this study focus on the 18 largest flood events in the Menomonee River basin from 1995 to 2010 (Table 3). We implement daily mean field bias correction (Smith and Krajewski 1991; Krajewski and Smith 2002) using the network of 21 MMSD rain gauges to improve the rainfall estimates by reflectivity-based radar. The daily bias correction takes the form:

$$B_i = \frac{\sum_{S_i} G_{ij}}{\sum_{S_i} R_{ij}}, \tag{1}$$

where G_{ij} is the daily rainfall accumulation for gauge j on day i, R_{ij} is the daily rainfall accumulation for the radar pixel containing gauge j on day i, and S_i is the index of the rain gauge stations from which both rain gauge and radar have positive rainfall accumulation for day i. The bias value is set to be different from 1.0 only if there are at least five positive radar–rain gauge pairs in the

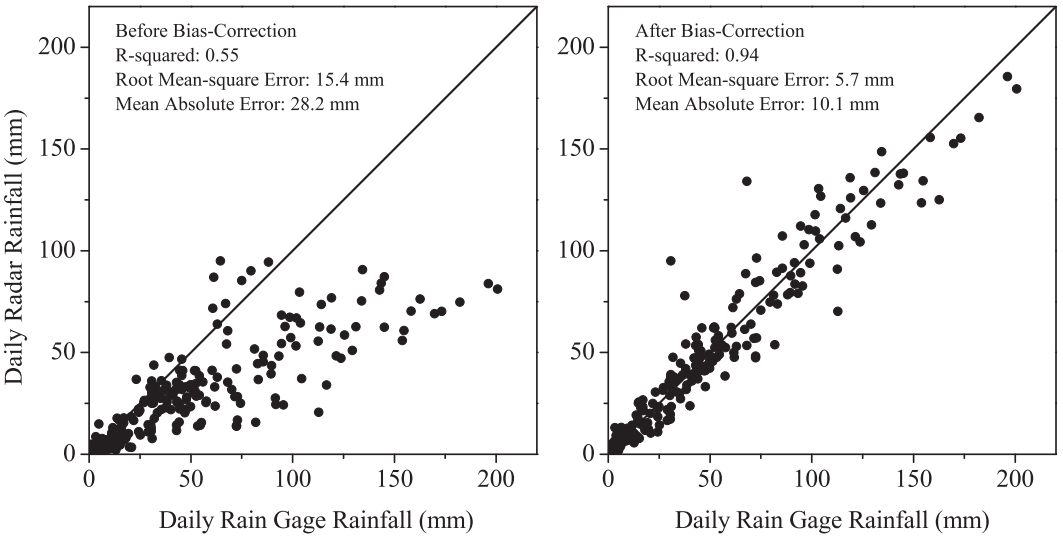

FIG. 2. Comparison of MMSD rain gauges and the corresponding radar–pixel daily rainfall accumulations (left) before and (right) after bias correction.

domain. Bias correction is implemented by multiplying each 15-min rainfall field on day i by B_i. The daily bias correction removes systematic bias due to variability in Z–R relationships and radar calibration errors (Villarini and Krajewski 2010). This bias correction procedure is the same as that used in Wright et al. (2012) and Smith et al. (2012).

The daily coefficient of determination (R^2) improved from 0.55 to 0.94 with bias correction (Fig. 2). The daily root-mean-square error (RMSE) decreased from 15.4 to 5.7 mm and the daily mean absolute error (MAE) from 28.2 to 10.1 mm. The improvements in radar rainfall estimates with multiplicative bias correction are consistent with previous studies showing that mean field bias correction is a key element in developing accurate rainfall products from conventional radar reflectivity measurements (Smith et al. 1996b; Seo et al. 1999; Krajewski and Smith 2002). Upgrading the U.S. weather radar network to include polarimetric capabilities provides the possibility of achieving comparable accuracy without mean field bias correction (Ryzhkov et al. 2005).

3. Results

a. Hydroclimatology of flooding

In this section, we examine the hydroclimatology of flooding through analyses of nonstationarities in flood magnitude and frequency in the Menomonee River and Cedar Creek basins (see the discussion of flood frequency analysis for nonstationary flood records in Villarini et al. 2009b). We conclude the section with an examination of nonstationarities in heavy rainfall frequency over the Milwaukee metropolitan region.

The nonparametric Mann–Kendall test (Mann 1945; Kendall 1975) was used throughout this paper to detect monotonic trends in flood and rainfall records. The magnitude of annual flood peaks in Honey Creek, Underwood Creek, and the downstream Menomonee River basin (Fig. 3, top and middle panels) show significant increasing trends since 1960 (at the 5% significance level). Changing flood peak magnitudes are particularly notable for large floods. In Honey Creek, nine of the top 10 flood peaks in a record of more than 50 years have occurred since 1997 (Fig. 3, middle). For the lower Menomonee River gauging station (Fig. 3, top), five of the largest seven flood peaks in a 50-yr record occurred in 1997, 1998, 2008, 2009, and 2010.

Flood peak magnitudes in the Menomonee River basin vary with drainage area and with the extent of urbanization. Honey Creek, the smallest and most intensely urbanized basin (Table 2), has five flood peaks with unit discharge greater than $4.0\,m^3\,s^{-1}\,km^{-2}$ since 2000 (Fig. 3, middle). Underwood Creek, which has an urban fraction of 92% (Table 2), has six flood peaks greater than $2.0\,m^3\,s^{-1}\,km^{-2}$ since 1997 (Fig. 3, middle). The lower Menomonee River gauging station has five flood peaks greater than $1.0\,m^3\,s^{-1}\,km^{-2}$, four of which have occurred since 1997 (Fig. 3, top), with the 21 June 1997 peak of $1.3\,m^3\,s^{-1}\,km^{-2}$ as the flood of record. Cedar Creek does not show significant trends (at the 5% significance level) in the magnitude of annual flood peaks in a record of 80 years. The record flood peak in Cedar Creek is $0.33\,m^3\,s^{-1}\,km^{-2}$, a factor of 4 smaller

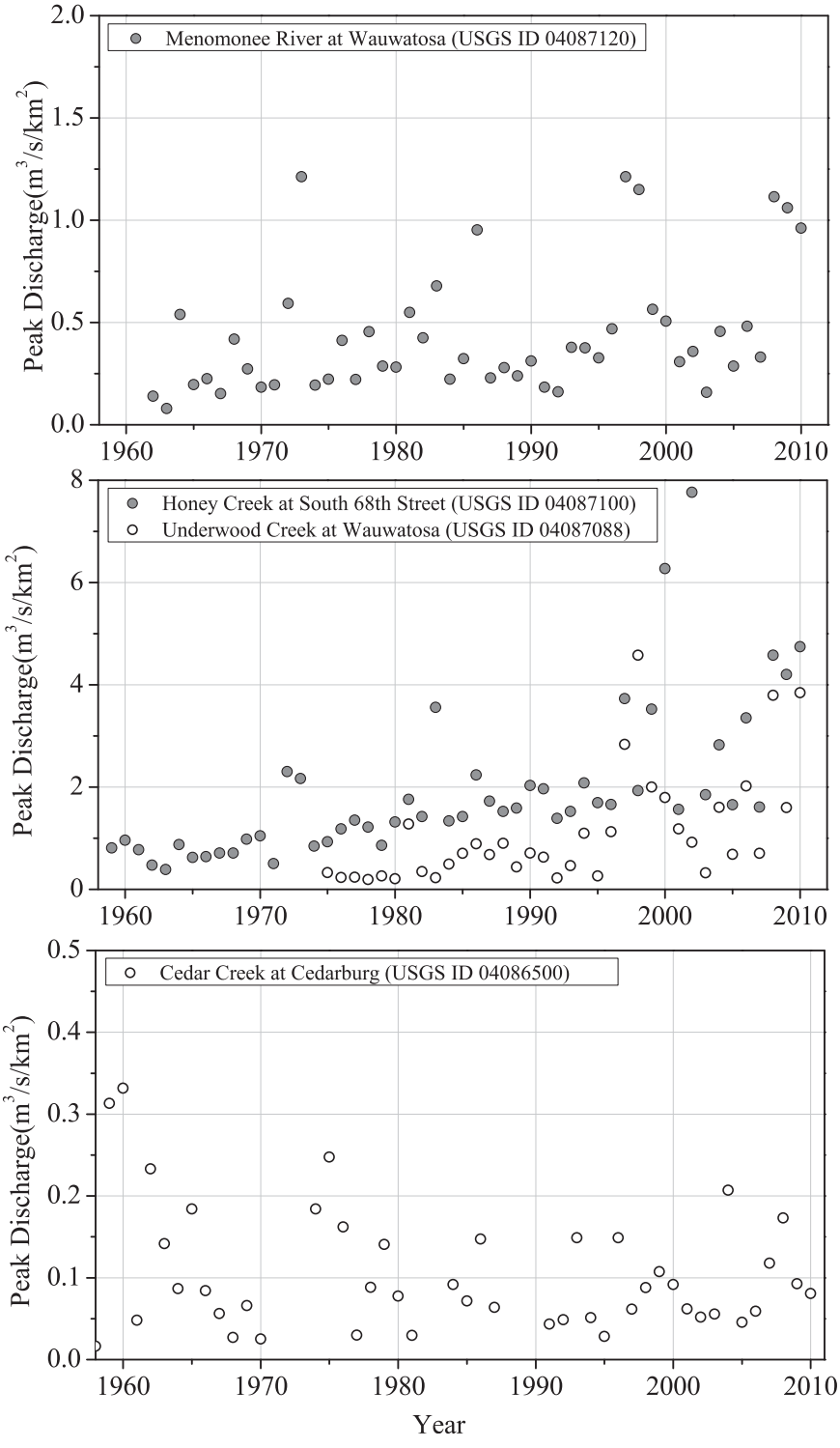

FIG. 3. Annual flood peaks (as a unit discharge in $m^3 s^{-1} km^{-2}$). (top) Menomonee River at Wauwatosa. (middle) Underwood Creek at Wauwatosa and Honey Creek at South 68th Street. (bottom) Cedar Creek near Cedarburg.

TABLE 4. The p values of Mann–Kendall trend tests for peak discharge series over different temporal periods.

USGS ID	Fixed period (1962–2010)	All available periods	Significance level
04087120	0.002	0.002 (1962–2010)	0.05
04087100	0.001	0.001 (1959–2010)	0.05
04087088	0.001	0.001 (1975–2010)	0.05
04086500	0.582	0.988 (1931–2010)	Not significant

than the record flood peak in the comparably sized Menomonee River. The two-sided p values and significance levels of Mann–Kendall tests for all peak discharge time series are summarized in Table 4.

In addition to nonstationarities in flood magnitude, we examined time trends in flood counts based on POT flood records for the Menomonee River and Cedar Creek basins. The threshold for each station was selected to provide an average of 4.2 flood events per year (e.g., Wright et al. 2012). A minimum interval of 2 days between peaks was chosen to ensure that multiple peaks within the ''same'' event are not treated as separate flood events. We also restrict consideration to 1962–2010, during which time the two basins have overlapping records. Flood counts in both the Menomonee River and Cedar Creek basins (Fig. 4) exhibit significant increasing trends at the 5% significance level (by means of Mann–Kendall test). By using the nonparametric Sen's estimator (Sen 1968), the linear trends of the flood peak counts are obtained. For the Menomonee River basin, flood peaks have increased by 3.5 events from 1961 to 2010, while the Cedar Creek basin experienced a total increase of 1.5 events during the same period.

The combined analyses of flood magnitudes and flood counts in Cedar Creek suggest that there is an increasing frequency of small floods, but the cumulative effect is not sufficient to produce a significant increase of annual flood peak magnitudes. These results are consistent with those of Villarini et al. (2013a), who found an increase in the frequency of POT events but not in the annual maximum flood peak magnitudes. We examine hydrologic processes that may play a role in changing flood counts in the Cedar Creek basin in section 3c.

The seasonality of annual flood peaks (Fig. 5) provides insights to changing flood regimes in the Menomonee River basin. In the bottom panel of Fig. 5, we show monthly flood peak counts for the Menomonee River and Cedar Creek during the period from 1962 to 2010. In the top panel, the same analyses are presented for the period from 1962 to 1981; the middle panel provides results for the 1982–2010 period. During the period from 1962 to 1981, both basins have similar seasonal distributions of flood peaks, in which March and April have the highest frequency of flood events. A shift in the seasonality of flood occurrence in the Menomonee basin is observed during the 1982–2010 period, during which most flood peaks are generated in JJA instead of in March and April, indicating a strong contribution from warm season thunderstorm systems (see detailed discussion of these issues in Ntelekos et al. 2007). The seasonality of flood peaks in Cedar Creek, however, remains unchanged.

To better understand flood-producing agents in the region, we examined the climatology of rainfall and snow cover using data (which covers the Menomonee River as well as Cedar Creek basin and extends from

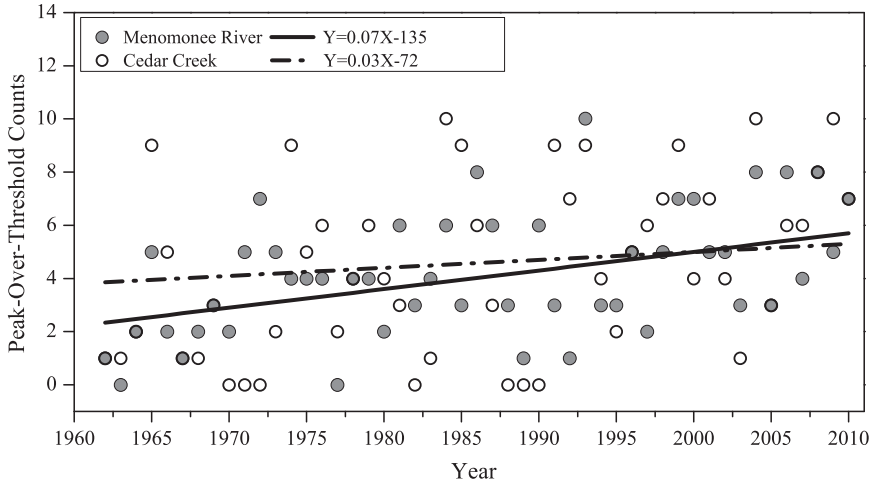

FIG. 4. Time series of annual flood peak counts over Menomonee River and Cedar Creek basins during 1962–2010. Trend lines are based on Sen's estimator and used to highlight the linear trends. Solid and dashed lines denote Menomonee River and Cedar Creek, respectively.

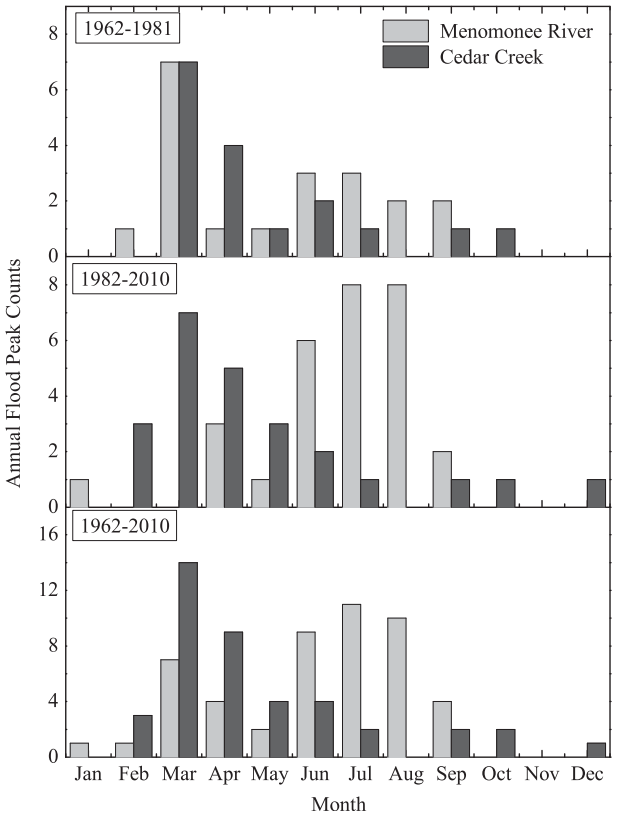

FIG. 5. Seasonality of annual flood peaks for Menomonee River and Cedar Creek over different time periods: (top) 1962–81, (middle) 1982–2010, and (bottom) 1962–2010.

1940 to 2010) from the National Climate Data Center (NCDC). Monthly maximum rainfall occurs during JJA, with median monthly rainfall ranging from 102 mm in June to 93 mm in August. Winter months (December–February) have the minimum rainfall during the year. The probability of snow cover in Milwaukee peaks in February, with a value of approximately 70% in early February, and decreases to approximately 40% by the beginning of March. At the end of March, the probability of snow cover is less than 10%. Rainfall increases sharply in April (with a median value of 85 mm). Thus, snowmelt may contribute directly in some cases to the flood regime of Cedar Creek and indirectly through elevated soil moisture associated with snowmelt.

Because of the shift of annual flood peak seasonality in the Menomonee River basin from March–April to JJA, it is not surprising to detect an increasing trend in the timing of the peaks (at the 10% significance level; Fig. 6). These results confirm the transition in the Menomonee from March–April floods to JJA floods. We do not detect significant trends in the timing of annual flood peaks for the Cedar Creek basin. Because flood peaks in Cedar Creek are associated with snowmelt and are due to the strong temperature dependence on snowmelt, it is likely that temperature increase will lead to significant trends in the timing of flood peaks in basins like Cedar Creek. This is not, however, a significant component of the flood hydroclimatology of flood record to date.

The frequency of heavy rainfall during the past two decades is examined based on hourly rainfall observations from 21 MMSD rain gauges. The hourly data have been aggregated to the daily scale. The number of days with daily rainfall accumulation exceeding 15 mm (an approximate value with 10% exceedance probability for most rain gauges) are computed for each year (Fig. 7). Although the variability of heavy rainfall days is large among the 21 gauges for certain years, the minimum, maximum, and mean values are consistently increasing

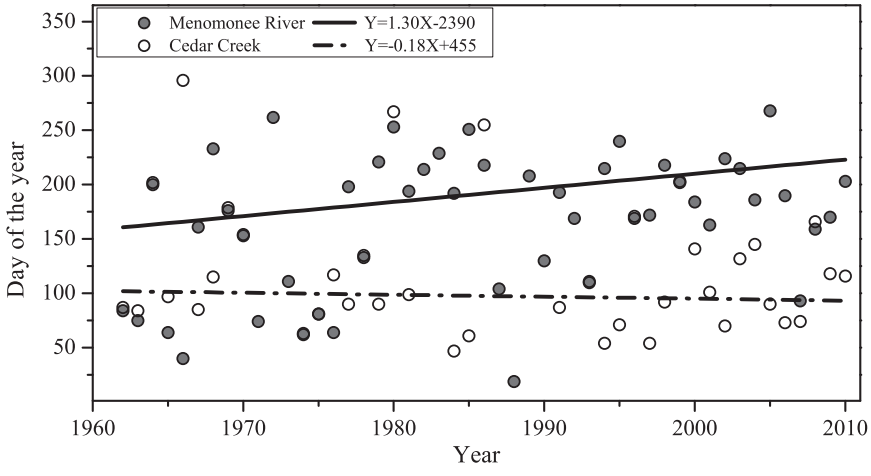

FIG. 6. Timing of the annual flood peaks in Cedar Creek and Menomonee River basin during 1962–2010. Lines are based on Sen's estimator and used to highlight the linear trends. Solid and dashed lines denote Menomonee River and Cedar Creek, respectively.

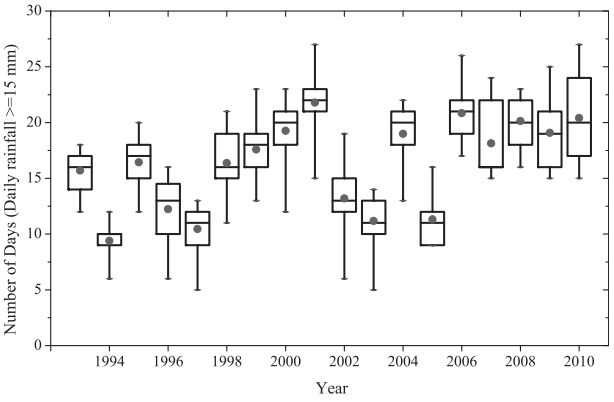

FIG. 7. Box plot of number of days with daily rainfall accumulation exceeding 15 mm during 1993–2010 for the network of 21 MMSD rain gauges. The line and dot within the box represent the median and mean values, respectively. The box spans the 0.25 and 0.75 quantiles, and the whiskers represent the minimum and maximum values.

(at the significance level of 5%), indicating an increasing heavy rainfall climatology over the Menomonee River basin during the past two decades. All of the heavy rainfall days occur during the warm season (May–September, figure not shown), which is consistent with the results of Villarini et al. (2011b).

b. *Hydrometeorology of flooding*

The hydrometeorology of flooding is examined through analyses of high-resolution, bias-corrected radar rainfall fields (see section 2) for the 18 flood events described in the following subsection. The 18 storms are all warm season thunderstorms, with occurrence times contained during the June–September time window (Table 3). There is a strong seasonal concentration for these storms during midsummer, with 16 of the 18 storms occurring in June and July.

A composite map of mean rainfall for the 18 storms (Fig. 8) shows a striking concentration of rainfall in the central portion of the Menomonee River basin. The maximum value of mean rainfall for the 18 storms exceeds 90 mm and is located downstream of the Little Menomonee and Menomonee Falls subbasins and upstream of the confluence of Underwood and Honey Creeks. Mean rainfall decreases sharply along the south–north direction of the basin, with a minimum of 54 mm on the northern boundary of the Menomonee basin. The gradients are very sharp to the west, with the abrupt increase in terrain marking the western margin of the rainfall maximum (Fig. 1). Mean rainfall varies more gradually to the east over Lake Michigan. Comparable spatial contrasts in warm season convective rainfall are described in Smith et al. (2012) for the Baltimore metropolitan region.

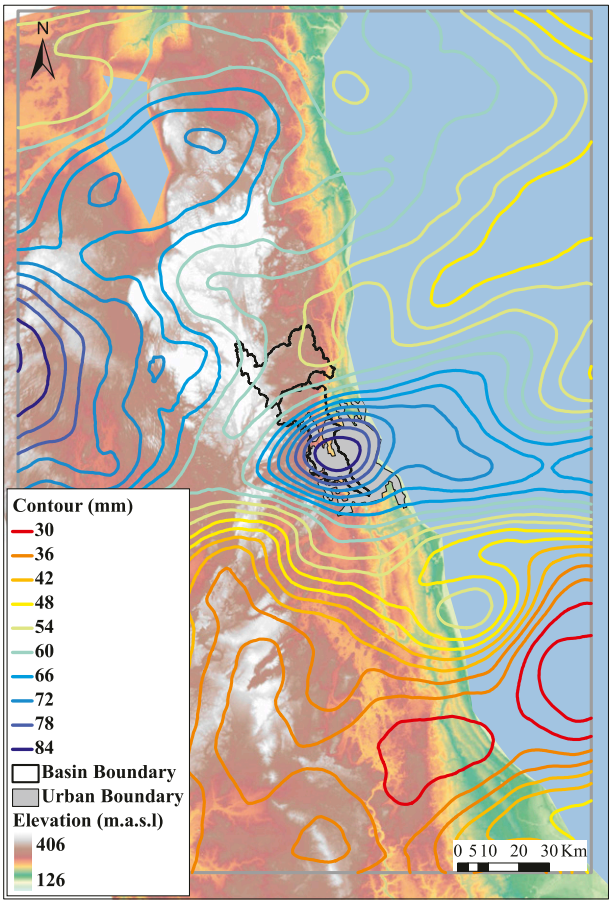

FIG. 8. Composite map of mean rainfall for the 18 largest flood-producing storms over the Menomonee River basin.

The storm total rainfall fields for the storms that produced the six largest flood peaks (see Table 3 for details) in the Menomonee River basin illustrate the systematic concentration of extreme rainfall over the Menomonee basin (Fig. 9). All six storms have maxima, or local maxima, in the central portion of the Menomonee River basin.

The largest spatial gradients in storm total rainfall occurred for the June 1997 and August 1998 storms. For the 21 June 1997 storm, which produced the flood of record for the Menomonee River at Wauwatosa, storm total rainfall ranged from 150 mm in the central portion of the basin to 75 mm along the northern boundary of the basin and 100 mm along the southern boundary (Fig. 9a). The most pronounced concentration of heavy rainfall for the central Menomonee basin occurred during the 8 August 1998 storm (Fig. 9b), with 150 mm over the central Menomonee, 3 times larger than the rainfall along the northern boundary of the basin and more than twice the rainfall along the southern boundary.

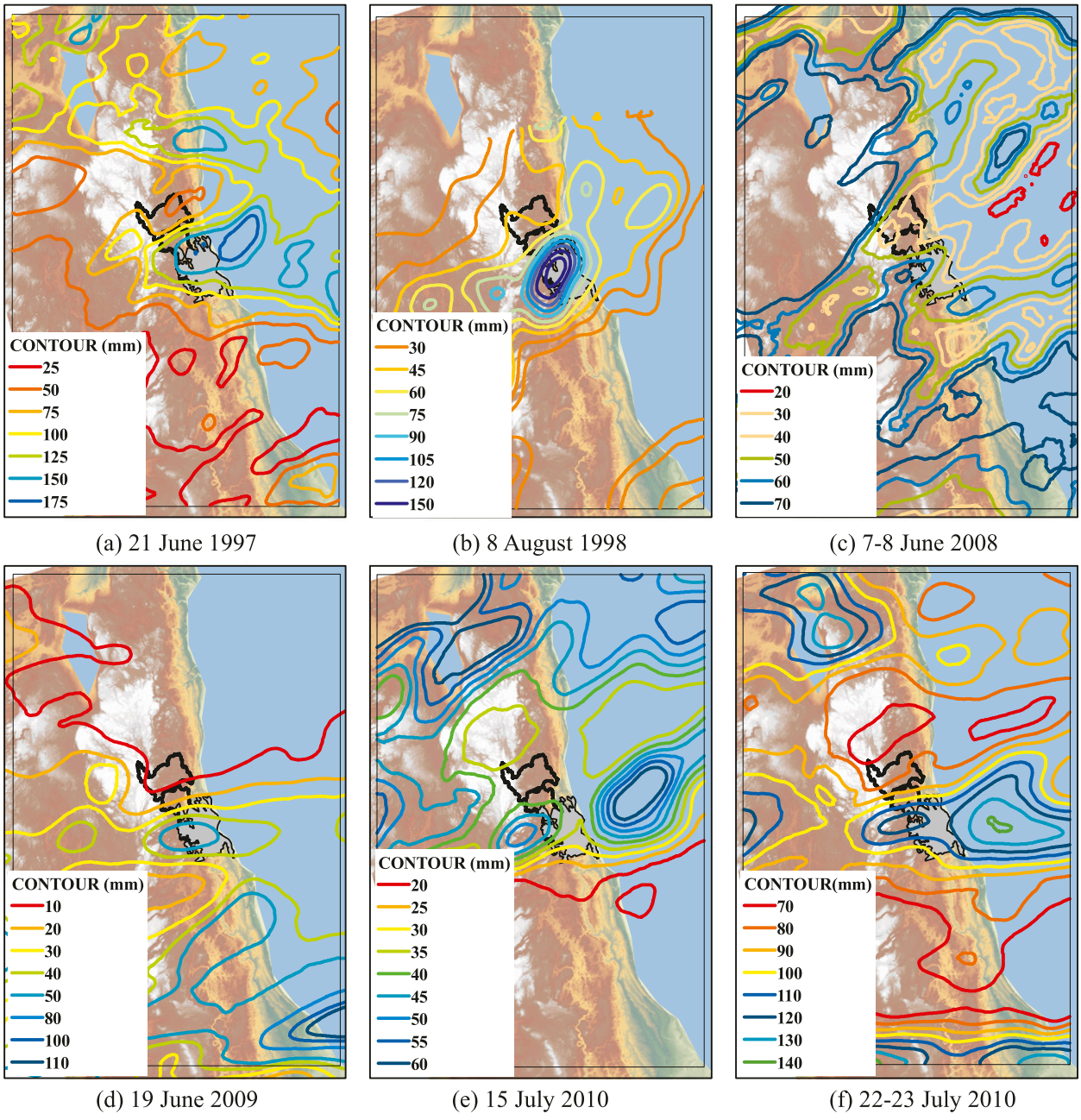

FIG. 9. Total rainfall map for six major storms: (a) 21 June 1997, (b) 8 August 1998, (c) 7–8 June 2008, (d) 19 June 2009, (e) 15 July 2010, and (f) 22–23 July 2010. Basin boundaries are shown in black lines. Milwaukee metropolitan region is shaded in gray.

Heavy rainfall in the Menomonee River basin for each of the six storms was embedded in a larger area of heavy rain. Heavy rainfall for the 7–8 June 2008 storm (Fig. 9c), as for most of the other storms, extended westward over the state of Wisconsin for more than 200 km, with rainfall maxima exceeding 200 mm in western Wisconsin. Like each of the six storms, the 7–8 June 2008 storm was a severe thunderstorm system and produced multiple tornadoes in western Wisconsin (figure not shown). The 22–23 July 2010 storm system also produced rainfall accumulations exceeding 200 mm in western Wisconsin. This storm was an organized thunderstorm system that moved rapidly over the Milwaukee metropolitan region from west to east. Each of the six storms has a dominant west to east component of motion (figure not shown).

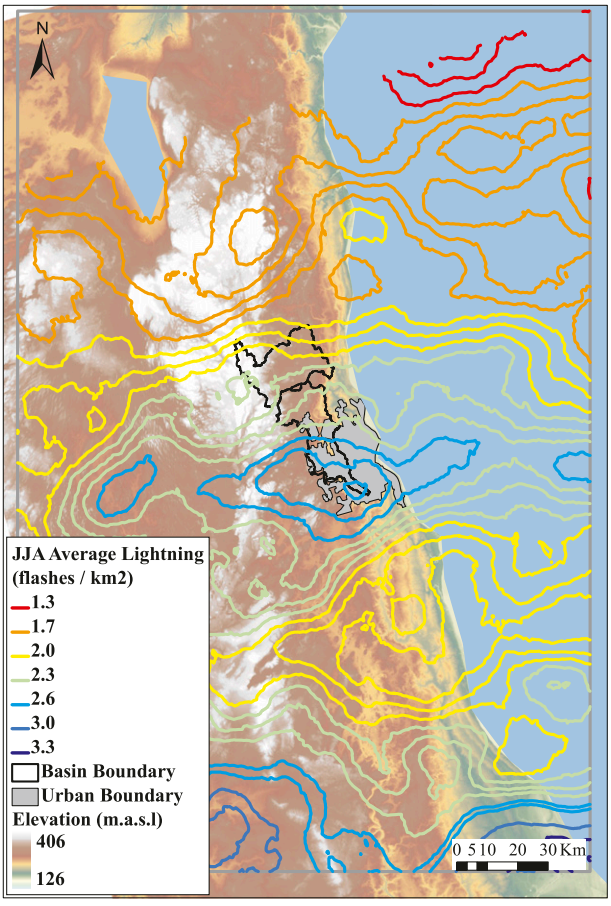

FIG. 10. Mean warm season (JJA) CG lightning flash density (flashes km^{-2}) over the Menomonee River basin.

The climatology of warm season (JJA) CG lightning frequency (Fig. 10) for the study region exhibits a local maximum over the Menomonee River basin. CG observations used in this study covered the period of 1995–2010, the same period as the 18 major storms. The maximum density of CG lightning flashes extend from the central to lower Menomonee River basin. The pattern of CG lightning density distribution, like the composite mean accumulated rainfall field for the 18 storms, exhibits a concentration over the metropolitan region and sharp gradients over the Milwaukee–Lake Michigan region.

c. *Flood hydrology*

We examine the flood hydrology of the Milwaukee metropolitan region through analyses of high-resolution radar rainfall fields and discharge for flood events in the Menomonee River basin. We present analyses for flood events during 1996–2010, based on flood peak magnitudes for the lower Menomonee River stream gauging station at Wauwatosa (see also composite hydrometeorological analyses in the previous subsection). During this period, discharge observations are also available at Underwood Creek and Menomonee Falls gauging stations. Underwood Creek is highly urbanized, and Menomonee Falls has only a small urbanized area concentrated near the outlet of the basin. Land use in the majority of the Menomonee Falls subbasin is similar to the adjacent Cedar Creek. We present analyses for four major flood events during the 2008–10 time period: 7–9 June 2008, 19 June 2009, 15 July 2010, and 22–23 July 2010. For the 2008–10 time period, two stream gauging stations in the Little Menomonee River and one station in Honey Creek are available, in addition to the lower Menomonee River, Underwood Creek, and Menomonee Falls stations.

1) RAINFALL-RUNOFF RELATIONSHIPS

To obtain our sample of flood events, we selected a peak discharge threshold for the Menomonee River at Wauwatosa ($0.38\,m^3\,s^{-1}\,km^{-2}$) that produced 18 floods (Table 3), for which WSR-88D radar rainfall observations were available. The flood discharge threshold provides a homogeneous population of warm season (June–September) flood events. For each of the 18 flood events, we computed peak discharge (expressed in Table 3 as a unit discharge in $m^3\,s^{-1}\,km^{-2}$), total runoff (mm) and total rainfall (mm), based on bias-corrected Hydro-NEXRAD rainfall fields (Table 3).

We examined runoff ratios (i.e., the ratio of runoff in millimeters to rainfall in millimeters) over a range of time scales. Figure 11 shows the relationships between maximum 3 and 24 h rainfall and runoff for the three basins. Runoff ratios at the 3-h scale for Underwood Creek have a median value of 0.30. By contrast, the median value of the runoff ratio at the 3-h scale for Menomonee Falls is 0.05. The 3-h runoff ratios for the full drainage basin represented by the Wauwatosa gauge have a median value of 0.20, smaller than the highly urbanized Underwood Creek, but 4 times as large as Menomonee Falls. The inferences from maximum 24-h runoff ratios are similar (Fig. 11, right). For Underwood Creek, the runoff ratios at 24-h scale range have a median value of 0.58, compared with the median value 0.17 in Menomonee Falls. Runoff ratios for Wauwatosa lie between those of the other two basins, with a median value of maximum 24-h runoff ratio of 0.43. The contrasts in maximum 3-h and maximum 24-h runoff ratios between the heavily urbanized portion of the Menomonee basin (represented by Underwood Creek) and the less urbanized portion of the watershed (represented by Menomonee Falls) reflect contrasts in both net runoff generation over the course of the storms and in the timing of flood response.

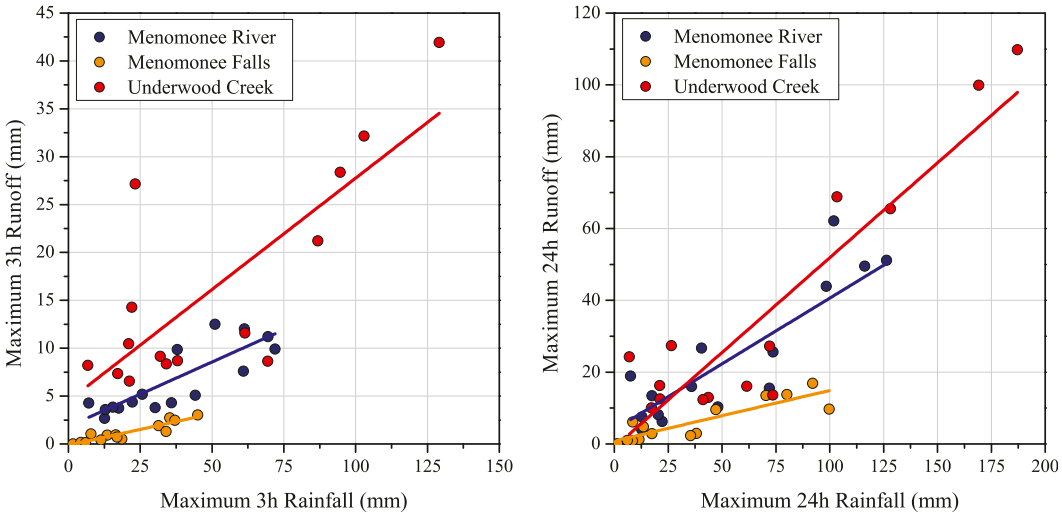

FIG. 11. Scatterplots of (left) maximum 3-h rainfall and runoff and (right) maximum 24-h rainfall and runoff for three basins: Menomonee River (blue dots), Menomonee Falls (orange dots), and Underwood Creek (red dots). Lines are used to highlight the linear relationship between the two variables.

Underwood Creek has much larger rainfall accumulations than Menomonee Falls for the 18 flood events. The median values at 1-, 3-, 6-, and 24-h periods for Underwood Creek range from 1.7 times larger than Menomonee Falls at 24-h time scale to more than twice as large at 6-h time scale (Table 5). For Underwood Creek, six of the 18 storms have 3-h rainfall accumulations greater than 50 mm, while for Menomonee Falls, no storms have rainfall accumulations greater than 50 mm (Fig. 11). Median rainfall accumulations in the entire Menomonee basin are smaller than values for Underwood Creek, but significantly larger than the values for Menomonee Falls, reflecting spatial heterogeneities in rainfall for flood-producing storms in the Menomonee River basin (see section 3b for additional analyses).

The contrasts in runoff among the three basins are even larger than for rainfall. At the 24-h time scale, median runoff in the lower Menomonee is 19 mm, 5 mm smaller than the median value for Underwood Creek, but more than 4 times larger than the median value for Menomonee Falls. The smallest 3-h runoff value of 7 mm in Underwood Creek among the 18 storms is 3 mm greater than the largest 3-h runoff value in Menomonee Falls (Fig. 11).

The variability of runoff and flood peak magnitudes across storm events exhibits qualitatively different behavior for the three basins than the results for median runoff (Table 5). Although Underwood Creek and the lower Menomonee River basin have higher variability in maximum 1-, 3-, 6-, and 24-h rainfall, the runoff variability is not correspondingly large, compared to the upper Menomonee River basin. The unitless coefficient of variation of flood peak magnitudes is 0.83 for Menomonee Falls, while Underwood Creek and Menomonee River basins are 0.50 and 0.45, respectively. Considering the large impervious fractions and compacted urban soils of Underwood Creek and Menomonee River, the dominant runoff generation mechanism is infiltration excess runoff (or Hortonian runoff), implying that the variability of flood peak discharge is mainly controlled by rainfall rate for the two subbasins. For Menomonee Falls, which has relatively low relief and extensive vegetated surfaces, saturation excess runoff production (or Dunne runoff), comes into play, such

TABLE 5. Median flood water balance for the 18 largest floods over three basins: Menomonee River, Underwood Creek, and Menomonee Falls. Quantities in parentheses are the dimensionless coefficients of variation.

		Max 1 h		Max 3 h		Max 6 h		Max 24 h	
Basins	Peak discharge ($m^3 s^{-1} km^{-2}$)	Runoff (mm)	Rainfall (mm)	Runoff (mm)	Rainfall (mm)	Runoff (mm)	Rainfall (mm)	Runoff (mm)	Rainfall (mm)
Menomonee River	0.48 (0.45)	2.1 (0.43)	20 (0.79)	4.4 (0.53)	30 (0.8)	7.2 (0.64)	37 (0.84)	19 (0.75)	41 (0.89)
Underwood Creek	1.60 (0.50)	5.7 (0.56)	25 (0.91)	10 (0.68)	34 (1)	12 (0.78)	38 (1.03)	24 (0.88)	62 (0.94)
Menomonee Falls	0.12 (0.83)	0.4 (0.85)	14 (0.74)	1.0 (0.85)	17 (0.75)	1.5 (0.89)	18 (0.85)	3.9 (0.94)	35 (0.88)

TABLE 6. Summary of the four major flood events. NA denotes missing data.

Events	Basins	Peak ($m^3 s^{-1} km^{-2}$)	Rainfall (mm)	Runoff (mm)	Runoff ratio (-)
7–9 Jun 2008	Menomonee River	1.12	165	98	0.59
	Honey Creek	3.25	160	159	0.99
	Underwood Creek	3.78	206	157	0.76
	Menomonee Falls	0.26	132	58	0.44
	Upper Little Menomonee	0.43	140	77	0.55
	Lower Little Menomonee	0.57	140	78	0.56
19 Jun 2009	Menomonee River	1.06	40	30	0.75
	Honey Creek	3.54	47	NA	NA
	Underwood Creek	1.59	46	17	0.36
	Menomonee Falls	0.12	25	3.8	0.15
	Upper Little Menomonee	0.06	34	3.8	0.11
	Lower Little Menomonee	0.17	34	8.7	0.25
15 Jul 2010	Menomonee River	0.87	103	35	0.34
	Honey Creek	3.02	93	50	0.54
	Underwood Creek	3.83	124	60	0.48
	Menomonee Falls	0.22	85	23	0.27
	Upper Little Menomonee	0.29	93	24	0.25
	Lower Little Menomonee	0.30	93	27	0.29
22–23 Jul 2010	Menomonee River	0.96	125	72	0.58
	Honey Creek	2.89	144	NA	NA
	Underwood Creek	2.29	134	94	0.70
	Menomonee Falls	0.46	92	37	0.40
	Upper Little Menomonee	0.30	100	36	0.36
	Lower Little Menomonee	0.55	100	52	0.52

that flood peak variability is tied to both spatiotemporal variability of rainfall totals and spatial heterogeneities of urbanization in the watershed, as detailed below. The high variability in flood peak discharge and runoff volume illustrates the role that spatial heterogeneity of surface properties (tied with different runoff generation mechanisms) play in the basin flood response.

2) EVENT HYDROLOGIC RESPONSE

Analyses of four major flood events in the Menomonee River basin provide additional insights into the role of spatial heterogeneity of land surface processes and the variability of rainfall in time and space in shaping flood response in urban watersheds (Table 6, Fig. 12). Six gauged watersheds (the Menomonee River basin and its five subbasins listed in Table 2), which vary in area and land surface properties, are included in the analyses. We distinguish the upper drainage basins with relatively low urbanization (Menomonee Falls, upper and lower Little Menomonee River) from the highly urbanized subbasins in the lower watershed (Underwood Creek and Honey Creek). The four flood events reflect the major flood episodes during the recent period of elevated frequency of heavy rainfall (Fig. 7). Peak discharge, total rainfall, and total runoff are summarized for each event and for each subbasin in Table 6.

For each of the four flood events, the magnitudes of flood peaks in Underwood Creek and Honey Creek are much larger than those for Menomonee Falls and the Little Menomonee (Table 6). Underwood Creek and Honey Creek flood peaks range from 1.59 to $3.83\,m^3 s^{-1} km^{-2}$. Flood peaks for Menomonee Falls and the Little Menomonee basins are all less than $0.6\,m^3 s^{-1} km^{-2}$.

Flood peak magnitudes for Honey Creek and Underwood Creek are quite similar for the 15 July 2010 and 7–9 June 2008 storms ($3.0–4.0\,m^3 s^{-1} km^{-2}$) and for the 22–23 July 2010 storm ($2.5–3.0\,m^3 s^{-1} km^{-2}$), but differ substantially for the 19 June 2009 storm, for which the Honey Creek unit discharge peak is more than twice that of the Underwood Creek unit discharge peak. This highlights the conclusion that spatial variability of rainfall can be an important element of extreme flood response, even for the highly urbanized portion of the lower Menomonee basin.

Menomonee Falls exhibits a marked split in storm event response between the small urbanized portion of the basin concentrated near the outlet and the rest of the basin that has not undergone significant urbanization. The 22–23 July 2010 flood response provides the most striking example of this phenomenon. The flood peak of $0.46\,m^3 s^{-1} km^{-2}$ occurs earlier than the peaks for either of the highly urbanized Underwood or Honey Creek basins and occurs within 30 min of the peak rainfall rate (Fig. 12d). A gradual rise produces a secondary peak more than 24 h after the initial peak. Similar response is

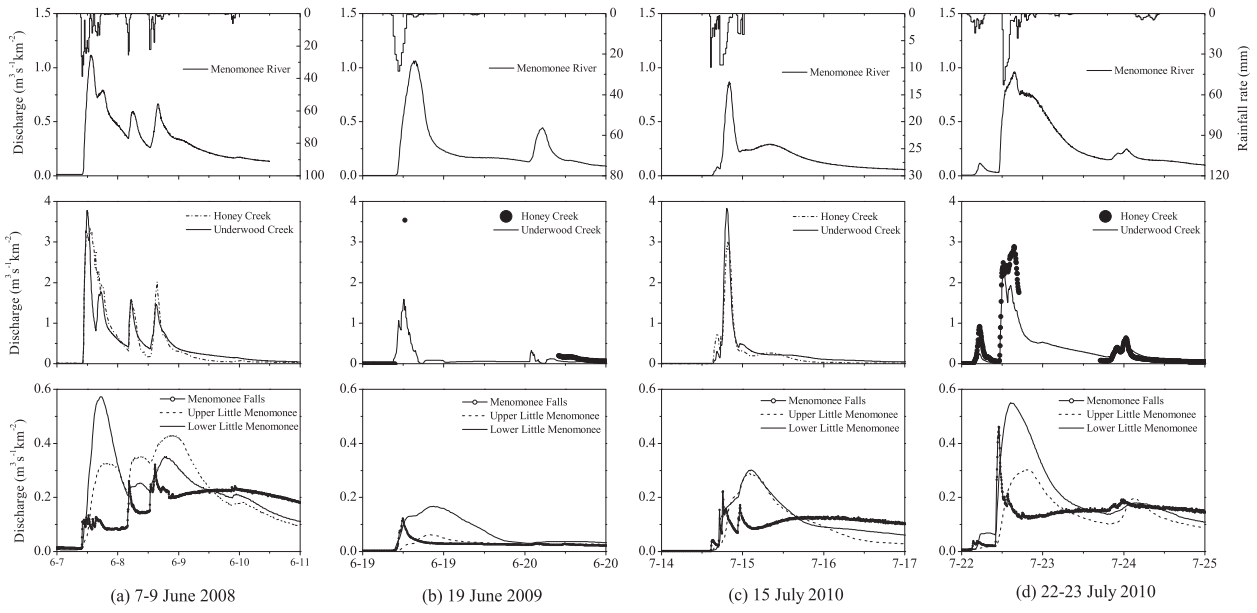

FIG. 12. Time series of bias-corrected, basin-averaged rainfall and discharge four major flood events: (a) 7–9 June 2008, (b) 19 June 2009, (c) 15 July 2010, and (d) 22–23 July 2010, showing (top) time series of rainfall and unit discharge for Menomonee River, (middle) unit discharge for Underwood Creek and Honey Creek, and (bottom) discharge for upper Little Menomonee River, lower Little Menomonee River, and Menomonee Falls. Discharge data are not complete for Honey Creek during 19 June 2009 and 22–23 July 2010.

seen for each of the four flood events in Menomonee Falls (Fig. 12). There is, for example, a sequence of peaks associated with each of the major pulses of rain from the 7–9 June 2008 storm period (Fig. 12a).

The flood peaks produced by the small urbanized fraction in Menomonee Falls provide insight into the mechanisms associated with increasing flood counts in Cedar Creek (Fig. 4). A moderate increase in urbanization can increase the number of small peaks in a drainage basin. For Cedar Creek, urbanization is not sufficiently extensive that the urban contribution makes a significant contribution to the magnitudes of annual flood peaks, which are still dominated by March–April events. There are, however, increasing frequencies of ''small'' flood peaks associated with fast response from the urbanizing portions of the watershed.

Rainfall variability, in particular the timing of maximum rainfall rate, plays a key role in determining flood peak response for the urban portion of the Menomonee watershed. The 7–9 June 2008 peaks in Underwood and Honey Creek, for example, follow the initial period of rainfall, which includes the highest rain rates during the storm (Fig. 12a). The extended period of heavy rainfall following the initial pulse of heavy rain produces subsequent smaller peaks, but these are not relevant to peak response at Wauwatosa for the flood event.

The urban flood response to the 7–9 June 2008 rainfall contrasts with flood response in the Little Menomonee and Menomonee Falls subbasins. The peak discharge in the lower Little Menomonee results from the first rainfall pulse. The peak for the upper Little Menomonee is from the last of three rainfall pulses, and the peak magnitude increases for each of the three pulses. For the final pulse, the unit discharge peak for the upper Little Menomonee exceeds the unit discharge peak from the lower Little Menomonee; this does not occur for any other events. The Menomonee Falls peak is for the last pulse but reflects the urban contribution (see discussion above) superimposed on slowly increasing nonurban flood response. The 7–9 June 2008 flood response in the Menomonee River basin again highlights two different runoff generation mechanisms in a watershed. For the urban portion of the watershed, Hortonian runoff dominates and flood response is dictated by short-term rainfall rates. For the nonurban portion of the watershed, runoff is generated by first reaching saturation in the soil column (Dunne runoff) resulting in slower response and flood peak magnitudes that are mainly controlled by the cumulative rainfall.

Flood response for the Menomonee basin at the 319 km^2 scale, represented by the Wauwatosa stream gauging station, reflects the heterogeneities in runoff production described above and the variability of rainfall in space and time. The 15 July 2010 flood response at Wauwatosa is characterized by unusually rapid rise

and decay of discharge (Fig. 12c), closely reflecting the Underwood and Honey Creek contributions. For the 22–23 July 2010 flood event, Menomonee Falls and the Little Menomonee contribute to peak response at Wauwatosa. The response of the Menomonee at Wauwatosa closely reflects details of the Honey Creek peak response, with a sharp rise, brief pause and slower increase to the peak discharge. The Little Menomonee peak for the June 2008 storm is comparable to the 22 July 2010 peak, but unlike 22 July 2010, the Little Menomonee peak occurred substantially later than the Wauwatosa peak and consequently did not contribute to downstream flood response. The spatial pattern of urbanization and rainfall rate variability combine to create a complex set of processes controlling flood peak response for the lower Menomonee.

4. Discussion

The striking transition in the seasonality of annual flood peaks in the Menomonee River basin is consistent with urbanization impacts on runoff production mechanisms due to increasing impervious area and decreased response times associated with elaboration of the drainage network through the storm drain system (see, e.g., Smith et al. 2002; Ntelekos et al. 2007). The role of warm season thunderstorms, which have large rainfall rates relative to other storms, is enhanced as urban flood agents as impervious cover increases and the storm drain network increases drainage density. The changing seasonal distribution of flood peaks may also be linked to modification of the heavy rainfall climatology by urbanization. Analyses in the previous section (see, in particular, Figs. 8–10) suggest that the sharp concentration of rainfall for flash flood–producing storms in the Menomonee River basin is linked to spatial heterogeneities in the structure and evolution of organized thunderstorm systems over the region. The resulting hypothesis is that urban modification of heavy rainfall through UHI, urban canopy, or urban aerosol effects (see Shepherd 2005) plays a significant role in the hydroclimatology of flooding for the Milwaukee metropolitan region. Of particular interest is the role of circulation anomalies associated with interactions between lake breeze from the Lake Michigan and UHI properties induced by urbanization in Milwaukee. Yang et al. (2013) have carried out a numerical modeling study over the Milwaukee–Lake Michigan region and showed that the UHI can enhance the intrusion of the lake breeze. The associated formation of a convergence zone over the urban region provides a mechanism for increasing rainfall over the city relative to the surrounding area. Additional research will be carried out to further address the role of urban land cover in modifying the regional climatology of flash flood–producing storms.

5. Summary and conclusions

The hydroclimatology, hydrometeorology, and hydrology of urban flooding are examined through analyses of rainfall, runoff, and flood peak magnitudes for the Milwaukee metropolitan region. We focus on nonstationarities of floods associated with the alterations of land surface processes and the regional climatology of heavy rainfall linked to urbanization. The major findings of this paper are as follows.

1) Both annual flood peak magnitudes and flood frequency have increased for the Menomonee River basin during the past five decades. During this period, the Menomonee River basin has also experienced a transition of flood events dominated by snowmelt to a regime in which warm season thunderstorms are the dominant flood agents. The agricultural ''reference'' watershed, Cedar Creek, has not seen a significant increase in flood magnitudes. The flood regime of Cedar Creek is dominated by March–April events (linked to the effects of snowmelt) and there is no evidence of changing seasonality of peaks. There is, however, an increase in the annual counts of POT flood events. A possible explanation is an increased frequency of small flood events associated with modest urbanization in Cedar Creek. This interpretation is consistent with the storm event hydrologic analyses of gauged watersheds in the Menomonee basin that have experienced only modest urbanization.
2) Analyses of rain gauge observations for the Milwaukee area over the past 20 years suggest that annual counts of heavy rainfall events (daily rainfall accumulations exceeding 15 mm) have increased significantly over the study region. These events are concentrated during the warm season and include a sequence of years from 2006 to 2010 with elevated counts of heavy rainfall events and major flood events. As noted below, there is a large spatial heterogeneity in flood-producing rainfall in the Milwaukee metropolitan area, which (see item 4 below) may also be linked to the temporal trends in heavy rainfall.
3) The spatial distribution of rainfall totals from storms that produce flood peaks in the Menomonee basin exhibit striking spatial heterogeneities. The mean storm total rainfall field for the 18 largest flood events in the Menomonee basin has a maximum of approximately 90 mm in the center of the basin and drops to 54 mm in less than 20 km along the south–north axis of the basin. Rainfall analyses for the six

largest flood events demonstrate that the rainfall maximum over the central Menomonee basin is an important element of the flood regime for the region. The spatial distribution of warm season (JJA) CG lightning flash density (1995–2010) also exhibits a maximum over the Menomonee River basin. These results suggest that urban modification of heavy rainfall may play an important role in the regional flood regime. Future studies will examine whether trends in heavy rainfall and its spatial heterogeneities are tied to urban modification of warm season thunderstorm systems.

4) Storm event hydrologic response in the Menomonee basin varies markedly with land surface properties that affect runoff production. The densely urbanized Underwood Creek exhibits larger flood peak discharge and runoff than the Menomonee River above Menomonee Falls, which has experienced only modest urbanization. A notable element of the contrasts in storm event hydrologic response between Underwood Creek and Menomonee Falls is the variation in rainfall, with Underwood Creek having markedly larger accumulations and higher short-duration rainfall rates. Analyses of rainfall and discharge observations in the Menomonee basin for the four major flood events in the 2008–10 time period highlight the role of spatial heterogeneities of hydrologic processes for urban flood response. The spatial pattern of urbanization interacts with rainfall distribution to control the scale-dependent flood peak responses in the Menomonee River basin.

The changes of flood response in a heterogeneous region highlight the interplay of large-scale climate change, regional climate change induced by urbanization, and contrasting runoff generation mechanisms associated with land surface properties. Assessing nonstationarities in flood hydrology will increasingly require the ability to distinguish the effects of global climate change, regional climate change, and changing land surface hydrologic responses associated with urbanization. Because of the large uncertainty of climate variability and limited in situ observations, we are not able to quantify the influence of large-scale climate variability on rainfall climatology in this study. For urbanized basins, like those in the Milwaukee metropolitan region, land surface processes can alter the types of storm systems that are dominant flood agents. In the urbanizing Milwaukee metropolitan region, the transformation is from snowmelt to organized warm season thunderstorm systems. Spatial patterns and temporal trends of heavy rainfall climatology can also be connected with urbanization. Urban modification of rainfall is one of the critical problems to address in assessing nonstationarities in urban flooding.

Acknowledgments. This study was supported by the National Science Foundation (NSF Grant CBET-1058027), the National Science Foundation of China (NSFC 51179084, 51190092), the special foundation of the Ministry of Water Resources, China (Project 201001004), the Willis Research Network, and the NOAA Cooperative Institute for Climate Science. NLDN data were provided by the NASA Lightning Imaging Sensor (LIS) instrument team and the LIS data center via the Global Hydrology Resource Center (GHRC) located at the Global Hydrology and Climate Center (GHCC), Huntsville, Alabama, through a license agreement with Global Atmospherics, Inc. (now Vaisala). The data available from the GHRC are restricted to LIS science team collaborators and to NASA EOS and TRMM investigators.

REFERENCES

Angel, J. R., and F. A. Huff, 1997: Changes in heavy rainfall in Midwestern United States. *J. Water Resour. Plan. Manage.,* **123,** 246–249.

Baeck, M. L., and J. A. Smith, 1998: Rainfall estimation by the WSR-88D for heavy rainfall events. *Wea. Forecasting,* **13,** 416–436.

Bentley, M. L., and J. A. Stallins, 2005: Climatology of cloud-to-ground lightning in Georgia, USA. *Int. J. Climatol.,* **25,** 1979–1996.

Borga, M., F. Tonelli, R. J. Moore, and H. Andrieu, 2002: Long-term assessment of bias adjustment in radar rainfall estimation. *Water Resour. Res.,* **38,** 1226, doi:10.1029/2001WR000555.

Bornstein, R., and Q. Lin, 2000: Urban heat islands and summertime convective thunderstorms in Atlanta: Three case studies. *Atmos. Environ.,* **34,** 507–516.

Carey, L. D., and S. A. Rutledge, 2003: Characteristics of cloud-to-ground lightning in severe and nonsevere storms over the central United States from 1989 to 1998. *J. Geophys. Res.,* **108,** 4483, doi:10.1029/2002JD002951.

——, ——, and W. A. Petersen, 2003: The relationship between severe storm reports and cloud-to-ground lightning polarity in the contiguous United States from 1989 to 1998. *Mon. Wea. Rev.,* **131,** 1211–1228.

Changnon, S. A., 1980: Evidence of urban and lake influences on precipitation in the Chicago area. *J. Appl. Meteor.,* **19,** 1137–1159.

——, and M. Demissie, 1996: Detection of changes in streamflow and floods resulting from climate fluctuations and land use-drainage changes. *Climatic Change,* **32,** 411–421.

——, F. A. Huff, and R. G. Semonin, 1971: METROMEX: An investigation of inadvertent weather modification. *Bull. Amer. Meteor. Soc.,* **52,** 958–967.

Cheng, C. K. M., and J. C. L. Chan, 2012: Impacts of land use changes and synoptic forcing on the seasonal climate over the Pearl River delta of China. *Atmos. Environ.,* **60,** 25–36.

Chung, E.-S., K. Park, and K. S. Lee, 2011: The relative impacts of climate change and urbanization on the hydrological response of a Korean urban watershed. *Hydrol. Processes,* **25,** 544–560.

Ciach, G. J., and W. F. Krajewski, 1999: On the estimation of radar rainfall error variance. *Adv. Water Resour.,* **22,** 585–595.

Claessens, L., C. Hopkinson, E. Rastetter, and J. Vallino, 2006: Effect of historical changes in land use and climate on the water budget of an urbanizing watershed. *Water Resour. Res.,* **42,** W03426, doi:10.1029/2005WR004131.

Collier, C., 2005: The impact of urban areas on weather. *Quart. J. Roy. Meteor. Soc.,* **132,** 1–25.

Cuo, L., D. P. Lenttenmaier, M. Alberti, and J. E. Richy, 2009: Effects of a century of land cover and climate change on the hydrology of the Puget Sound basin. *Hydrol. Processes,* **23,** 907–933.

Dixon, P. G., and T. L. Mote, 2003: Patterns and causes of Atlanta's urban heat island-initiated precipitation. *J. Appl. Meteor.,* **42,** 1273–1284.

Doswell, C. A., H. E. Brooks, and R. A. Maddox, 1996: Flash flood forecasting: An ingredients-based methodology. *Wea. Forecasting,* **11,** 560–581.

Easterling, D. R., G. A. Meehl, C. Parmesan, S. A. Changnon, T. R. Karl, and L. O. Mearns, 2000: Climate extremes: Observations, modeling, and impacts. *Science,* **289,** 2068–2074.

Franczyk, J., and H. Chang, 2009: The effects of climate change and urbanization on the runoff of the rock creek basin in the Portland metropolitan area, Oregon, USA. *Hydrol. Processes,* **23,** 805–815.

Fulton, R., J. P. Breidenbach, D. J. Seo, D. A. Miller, and T. O'Bannon, 1998: The WSR-88D rainfall algorithm. *Wea. Forecasting,* **13,** 377–398.

Hejazi, M. I., and M. Markus, 2009: Impacts of urbanization and climate variability on floods in northeastern Illinois. *J. Hydrol. Eng.,* **14,** 606–616.

Held, I. M., and B. J. Soden, 2006: Robust responses of the hydrological cycle to global warming. *J. Climate,* **19,** 5686–5699.

Hewlett, J. D., and J. D. Helvey, 1970: Effects of forest clear-felling on the storm hydrograph. *Water Resour. Res.,* **6,** 768–782.

Solomon, S., D. Qin, M. Manning, M. Marquis, K. Averyt, M. M. B. Tignor, H. L. Miller Jr., and Z. Chen, Eds., 2007: *Climate Change 2007: The Physical Science Basis.* Cambridge University Press, 996 pp.

Karl, T. R., and R. W. Knight, 1998: Secular trends of precipitation amounts, frequency, and intensity in the USA. *Bull. Amer. Meteor. Soc.,* **79,** 231–241.

Kendall, M. G., 1975: *Rank Correlation Methods.* Charles Griffin, London.

Krajewski, W. F., and J. A. Smith, 2002: Radar hydrology: Rainfall estimation. *Adv. Water Resour.,* **25,** 1387–1394.

——, and Coauthors, 2010: Towards better utilization of NEXRAD data in hydrology: An overview of Hydro-NEXRAD. *J. Hydroinf.,* **13,** 255–266.

Kunkel, K. E., K. Andsager, and D. R. Easterling, 1999: Long-term trends in extreme precipitation events over the coterminous United States and Canada. *J. Climate,* **12,** 2515–2527.

Lei, M., D. Niyogi, C. Kishtawal, R. A. Pielke, A. Beltran-Przekurat, T. E. Nobis, and S. S. Vaidya, 2008: Effect of explicit urban land surface representation on the simulation of the 26 July 2005 heavy rain event over Mumbai, India. *Atmos. Chem. Phys.,* **8,** 5975–5995.

Lettenmaier, D. P., E. F. Wood, and J. R. Wallis, 1994: Hydro-climatological trends in the continental United States, 1948–88. *J. Climate,* **7,** 586–607.

Lin, C.-Y., W.-C. Chen, P.-L. Chang, and Y.-F. Sheng, 2011: Impact of the urban heat island effect on precipitation over a complex geographic environment in northern Taiwan. *J. Appl. Meteor. Climatol.,* **50,** 339–353.

Lo, J. C. F., A. K. H. Lau, F. Chen, J. C. H. Fung, and K. K. M. Leung, 2007: Urban modification in a mesoscale model and the effects on the local circulation in the Pearl River delta region. *J. Appl. Meteor. Climatol.,* **46,** 457–476.

Lowry, W. P., 1998: Urban effects on precipitation amount. *Prog. Phys. Geogr.,* **22,** 477–520.

Mann, H. B., 1945: Non-parametric tests against trend. *Econometrica,* **13,** 245–259.

Merz, R., 2003: A process typology of regional floods. *Water Resour. Res.,* **39,** 1340, doi:10.1029/2002WR001952.

Miao, S., F. Chen, Q. Li, and S. Fan, 2011: Impacts of urban processes and urbanization on summer precipitation: A case study of heavy rainfall in Beijing on 1 August 2006. *J. Appl. Meteor. Climatol.,* **50,** 806–825.

Milly, P. C. D., J. Betancourt, M. Falkenmark, R. M. Hirsch, Z. W. Kundzewicz, D. P. Lettenmaier, and R. J. Stouffer, 2008: Stationarity is dead: Whither water management? *Science,* **319,** 573–574.

Mote, T. L., M. C. Lacke, and J. M. Shepherd, 2007: Radar signatures of the urban effect on precipitation distribution: A case study for Atlanta, Georgia. *Geophys. Res. Lett.,* **34,** L20710, doi:10.1029/2007GL031903.

Ntelekos, A. A., J. A. Smith, and W. F. Krajewski, 2007: Climatological analyses of thunderstorms and flash floods in the Baltimore metropolitan region. *J. Hydrometeor.,* **8,** 88–101.

——, ——, M. L. Baeck, W. F. Krajewski, A. J. Miller, and R. Goska, 2008: Extreme hydrometeorological events and the urban environment: Dissecting the 7 July 2004 thunderstorm over the Baltimore, MD, metropolitan region. *Water Resour. Res.,* **44,** W08446, doi:10.1029/2007WR006346.

Praskievicz, S., and H. Chang, 2009: A review of hydrological modelling of basin-scale climate change and urban development impacts. *Prog. Phys. Geogr.,* **33,** 650–671.

Reed, S. M., and D. R. Maidment, 1999: Coordinate transformation for using NEXRAD data in GIS-based hydrologic modeling. *J. Hydrol. Eng.,* **4,** 174–182.

Ryzhkov, A. V., S. E. Giangrande, and T. J. Schuur, 2005: Rainfall estimation with a polarimetric prototype of WSR-88D. *J. Appl. Meteor.,* **44,** 502–515.

Semadeni-Davies, A., C. Hernebring, G. Svensson, and L.-G. Gustafsson, 2008a: The impacts of climate change and urbanisation on drainage in Helsingborg, Sweden: Combined sewer system. *J. Hydrol.,* **350,** 100–113.

——, ——, ——, and ——, 2008b: The impacts of climate change and urbanisation on drainage in Helsingborg, Sweden: Suburban stormwater. *J. Hydrol.,* **350,** 114–125.

Sen, P. K., 1968: Estimates of the regression coefficient based on Kendall's tau. *J. Amer. Stat. Assoc.,* **63,** 1379–1389.

Seo, B. C., W. F. Krajewski, A. Kruger, P. Domaszczynski, J. A. Smith, and M. Steiner, 2010: Radar-rainfall estimation algorithms of Hydro-NEXRAD. *J. Hydroinf.,* **13,** 277–291.

Seo, D. J., J. P. Breidenbach, and E. R. Johnson, 1999: Real-time estimation of mean field bias in radar rainfall data. *J. Hydrol.,* **223,** 131–147.

Shepherd, J. M., 2005: A review of the current investigations of urban-induced rainfall and recommendations for the future. *Earth Interact.,* **9,** doi:10.1175/EI156.1.

——, H. Pierce, and A. J. Negri, 2002: Rainfall modification by major urban areas: Observations from spaceborne rain radar on the TRMM satellite. *J. Appl. Meteor.,* **41,** 689–701.

——, M. Carter, M. Manyin, D. Messen, and S. Burian, 2010: The impact of urbanization on current and future coastal

precipitation: A case study for Houston. *Environ. Plann.,* **37B,** 284–304.

Sivapalan, M., 2005: Linking flood frequency to long-term water balance: Incorporating effects of seasonality. *Water Resour. Res.,* **41,** W06012, doi:10.1029/2004WR003439.

Smith, J. A., and W. F. Krajewski, 1991: Estimation of the mean field bias of radar rainfall estimates. *J. Appl. Meteor.,* **30,** 397–412.

——, M. L. Baeck, M. Steiner, and A. J. Miller, 1996a: Catastrophic rainfall from an upslope thunderstorm in the central Appalachian: The Rapidan storm of June 27, 1995. *Water Resour. Res.,* **32,** 3099–3113, doi:10.1029/96WR02107.

——, D. J. Seo, M. L. Baeck, and M. D. Hudlow, 1996b: An intercomparison study of NEXRAD precipitation estimates. *Water Resour. Res.,* **32,** 2035–2045, doi:10.1029/96WR00270.

——, M. L. Baeck, J. E. Morrison, P. Sturdevant-Rees, D. F. Turner-Gillespie, and P. D. Bates, 2002: The regional hydrology of extreme floods in an urbanizing drainage basin. *J. Hydrometeor.,* **3,** 267–282.

——, ——, K. L. Meierdiercks, P. A. Nelson, A. J. Miller, and E. J. Holland, 2005: Field studies of the storm event hydrologic response in an urbanizing watershed. *Water Resour. Res.,* **41,** W10413, doi:10.1029/2004WR003712.

——, ——, G. Villarini, and W. F. Krajewski, 2010: The hydrology and hydrometeorology of flooding in the Delaware River basin. *J. Hydrometeor.,* **11,** 841–859.

——, G. Villarini, and M. L. Baeck, 2011: Mixture distributions and the climatology of extreme rainfall and flooding in the eastern United States. *J. Hydrometeor.,* **12,** 294–309.

——, M. L. Baeck, G. Villarini, C. Welty, A. J. Miller, and W. Krajewski, 2012: Analyses of a long-term high-resolution radar rainfall data set for the Baltimore metropolitan area. *Water Resour. Res.,* **48,** W04504, doi:10.1029/2011WR010641.

Steiner, M., and J. A. Smith, 2002: Use of three-dimensional structure for automated detection and removal of non-precipitating echoes in radar data. *J. Atmos. Oceanic Technol.,* **19,** 673–686.

Tapia, A., J. A. Smith, and M. Dixon, 1998: Estimation of convective rainfall from lightning observations. *J. Appl. Meteor.,* **37,** 1497–1509.

Villarini, G., and W. F. Krajewski, 2010: Review of the different sources of uncertainty in single-polarization radar-based estimates of rainfall. *Surv. Geophys.,* **31,** 107–129.

——, F. Serinaldi, J. A. Smith, and W. F. Krajewski, 2009a: On the stationarity of annual flood peaks in the continental United States during the 20th century. *Water Resour. Res.,* **45,** W08417, doi:10.1029/2008WR007645.

——, J. A. Smith, F. Serinaldi, J. Bales, P. D. Bates, and W. F. Krajewski, 2009b: Flood frequency analysis for nonstationary annual peak records in an urban drainage basin. *Adv. Water Resour.,* **32,** 1255–1266.

——, ——, M. L. Baeck, and W. F. Krajewski, 2011a: Examining flood frequency distributions in the Midwest U.S. *J. Amer. Water Resour. Assoc.,* **43,** 447–463.

——, ——, ——, R. Vitolo, D. B. Stephenson, and W. Krajewski, 2011b: On the frequency of heavy rainfall for the Midwest of the United States. *J. Hydrol.,* **400,** 103–120.

——, ——, ——, B. K. Smith, and P. Sturdevant-Rees, 2013a: Hydrologic analyses of the July 17–18, 1996, flood in Chicago and the role of urbanization. *J. Hydrol. Eng.,* **18,** 250–259.

——, ——, and G. A. Vecchi, 2013b: Changing frequency of heavy rainfall over the central United States. *J. Climate,* **26,** 351–357.

Voss, R., W. May, and E. Roeckner, 2002: Enhanced resolution modelling study on anthropogenic climate change: Changes in extremes of the hydrological cycle. *Int. J. Climatol.,* **22,** 755–777.

Wright, D. B., J. A. Smith, G. Villarini, and M. L. Baeck, 2012: The hydroclimatology of flash flooding in Atlanta. *Water Resour. Res.,* **48,** W04524, doi:10.1029/2011WR011371.

Yang, G., L. C. Bowling, K. A. Cherkauer, B. C. Pijanowski, and D. Niyogi, 2010: Hydroclimatic response of watersheds to urban intensity: An observational and modeling-based analysis for the White River basin, Indiana. *J. Hydrometeor.,* **11,** 122–138.

Yang, L., J. A. Smith, M. L. Baeck, E. Bou-Zeid, S. M. Jessup, F. Tian, and H. Hu, 2013: Impact of urbanization on heavy convective precipitation under strong large-scale forcing: A case study over the Milwaukee–Lake Michigan region. *J. Hydrometeor.,* in press.

Zhang, C. L., S. G. Miao, Q. C. Li, X. Xia, and C. Y. Xuan, 2009: Impacts of urban expansion and future green planting on summer precipitation in the beijing metropolitan area. *J. Geophys. Res.,* **114,** D02116, doi:10.1029/2008jd010328.

Zhang, Y., and J. A. Smith, 2003: Space–time variability of rainfall and extreme flood response in the Menomonee River basin, Wisconsin. *J. Hydrometeor.,* **4,** 506–517.